21

Institute of Theoretical
and Experimental Physics

FERMILAB
SEP 29 1999

ITEP-11-99

V.Egorytchev, V.Saveliev

MONTE CARLO SIMULATION OF TRANSITION RADIATION AND ELECTRON IDENTIFICATION FOR HERA-B

Fermilab Library
0 1160 0070490 2

Moscow 1999

UDK 539.1 M-16

MONTE CARLO SIMULATION OF TRANSITION RADIATION AND ELECTRON IDENTIFICATION FOR HERA-B: Preprint ITEP 11-99/

V.Egorytchev, V.Saveliev - M., 1999 -20p.

Transition radiation detectors show the great promise for use in the identification of B decay products in heavy quark experiment at hadron beams. Monte Carlo simulation of Transition Radiation developed to perform the systematic analysis of the performances and optimization of Transition Radiation Detectors. Monte Carlo program of simulation TRD compatible with GEANT - Detector Description and Simulation Tool was developed for the full GEANT simulation analysis of HERA-B experiment at DESY. The results of the Monte Carlo calculation are in agreement with experimental data obtained with full scale prototype of TRD.

Fig. - 8, ref. - 18 name.

© Институт теоретической и экспериментальной физики, 1999

1 Introduction.

Lepton identification is one of the most crucial features of the experimental research of CP violation in system of B mesons, proposed on existing and future experiments in High Energy Physics. Neutral B meson system provides an important stringent test of the Standard Model (SM). Decay mode $B^0 \to J/\psi K_s^0$ is predicted to show large CP asymmetry with the strength directly related to the parameters of Cabibo-Kobayashi-Maskawa (CKM) matrix [1]. The main physics goal of the proposed experiments and HERA-B experiment is the CP - violation measurement in B decay modes with multiple final-state leptons, in particular the decay $B^0 \to J/\psi K_s^0 \to l^+l^-\pi^+\pi^-$, generally accepted as the best candidates, both theoretically and experimentally, for the study of CP asymmetries [2]. The initial flavor of the B meson decaying to $J/\psi K_s^0$ is tagged using the other b hadron, decaying semileptonicaly (lepton tag) or via the transition $b \to c \to s$ (kaon tag). Good lepton identification is a important conditions of $B^0 \to J/\psi K_s^0$ decay reconstruction, lepton tagging and the additional physics study. In this case the particle identification based on Transition Radiation can used as effectively experimental method for electron identification in proposed experiments.

2 Properties of Transition Radiation.

Transition radiation is the electro-magnetic radiation that is emitted when a charge particle verses the boundary between two media with different dielectric properties. In a simple explanation the field of charge approaching a boundary can be seen as superposition of the field of the charge inside the medium and the field of image charge on the other side of boundary [3]. As shown schematically in Fig. 1 the effect is strongly peaked in the forward direction and it is symmetric, i.e. the radiation emitted is the same whether the particle enters medium 2 from medium 1 or enters medium 1 from medium 2. In more formal terms transition radiation is the result of the reformation of the particles field when traveling from a medium with ϵ_1 to a medium with ϵ_2. The frequency spectrum of transition radiation emitted by a particle with charge e upon perpendicular traversal through a single interface between two media with dielectric constants ϵ_1 and ϵ_2 has been calculated by V.Ginzburg and I.Frank [3], and by G.Garibian [4]. For practically application the most interesting case is the Transition radiation emitted by relativistic particle to perform identification of particles with different mass or charges. The rel-

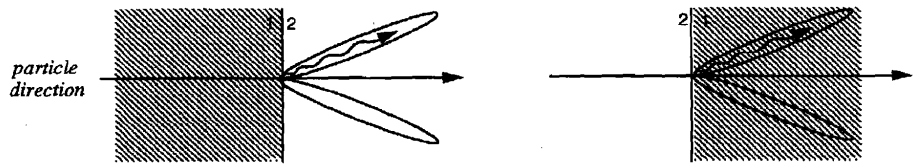

Figure 1. Transition Radiation is strongly peaked in to the forward direction and it symmetric, i. e. the radiation emitted is the same whether the particle enters medium 2 from medium 1 or enters medium 1 from medium 2.

atively simple expression have been found for the differential and the total radiation emitted at a single interface [5], where $\omega_{1,2}$ are the plasma frequencies of the two media, θ is emission angle of the photon with respect to the particle trajectory, and $\alpha = e^2/\hbar c$:

- the spectral dependence of transition radiation intensity:

$$\frac{d^2W}{d\omega d\theta} = \frac{2\alpha\hbar\theta^3}{\pi}\left(\frac{1}{1/\gamma^2+\theta^2+\omega_1^2/\omega^2} - \frac{1}{1/\gamma^2+\theta^2+\omega_2^2/\omega^2}\right) \quad (1)$$

- differential energy spectrum is describe:

$$\frac{d^2W}{d\omega} = \frac{\alpha\hbar}{\pi}\left[\left(\frac{\omega_1^2+\omega_2^2+2\omega^2/\gamma^2}{\omega_1^2-\omega_2^2}\right)\times\left(\frac{1/\gamma^2+\omega_1^2/\omega^2}{1/\gamma^2+\omega_2^2/\omega^2}\right)-2\right] \quad (2)$$

- the total intensity of radiation emitted at a single interface:

$$W = \int\int\left(d^2W d\omega d\theta\right) d\omega d\theta = \frac{\alpha\hbar}{\pi}\frac{(\omega_1-\omega_2)^2}{\omega_1+\omega_2}\gamma \quad (3)$$

From this equations are predicted some remarkable features for transition radiation (for relativistic case) [6]:

- the total energy lost by transition radiation is increases proportional to the Lorentz factor γ ($\gamma = E/m_0c^2$) of particle, essentially due to the fact that the photon spectrum becomes harder with increasing γ. It shows that linear dependence with γ can be used to discriminate between single charged particles with similar momentum but different mass;
- the most of the emission takes place within a cone of half angle $1/\gamma$, which for highly relativistic particles means practically along the particle axis;

- the electrodynamic nature of the transition radiation indicates that in an interface as have seen from the above equations the probability between media with different dielectric constants, the number of photons is of the order of $\alpha = 1/137$.
- for highly relativistic particles most of the radiation is emitted in the X-ray region.

On Fig. 2 are present the yield/$\hbar\omega$ - Production Spectrum (dashed line) for a single interface as a function of the TR photon energy [7]. The emission spectrum can be divided into three parts:

- for a large TR photon energy (typically > 30 keV) $\omega > \gamma\omega_2$ is observe a large drop of the intensity;
- for medium energies, $\gamma\omega_1 < \omega < \gamma\omega_2$ have the logarithmic decrease with photon frequency ω;
- for small energies $\omega < \gamma\omega_1 = 1$ keV, the yield is almost constant.

3 Operation principles and particle identification with Transition Radiation.

3.1 Multiple interfaces (radiator).

As we have seen from the above equation the probability of emission of photons is very small $\sim 10^{-2}$ and should be enhanced for experimental studies. For practical purpose is very important effect of the positive interference between the radiation emitted at many interfaces, it is possible to enhance the effect enough to build an identification detector [7]. This could be realized by to take many such interfaces usually realized by the stack (radiator foils). In this case, interference effects between the individual interfaces of the radia tor must be taken to account, leading to modulation of the frequency distribution obtained from a single interface and for high values of γ ,to a saturation the yield. The differential spectrum of X-ray transition radiation for a periodic radiator of N foils with thickness l_1 and spacing l_2 is given by

$$\frac{d^2W_N}{d\theta d\omega} = \frac{d^2W_0}{d\theta d\omega} 4sin^2\left(\frac{l_1}{Z_1}\right)\frac{sin^2[N(l_1/Z_1 + l_2/Z_2)]}{sin^2(l_1/Z_1 + l_2/Z_2)} \tag{4}$$

where Z_1 and Z_2 are the formation zones for the two media:

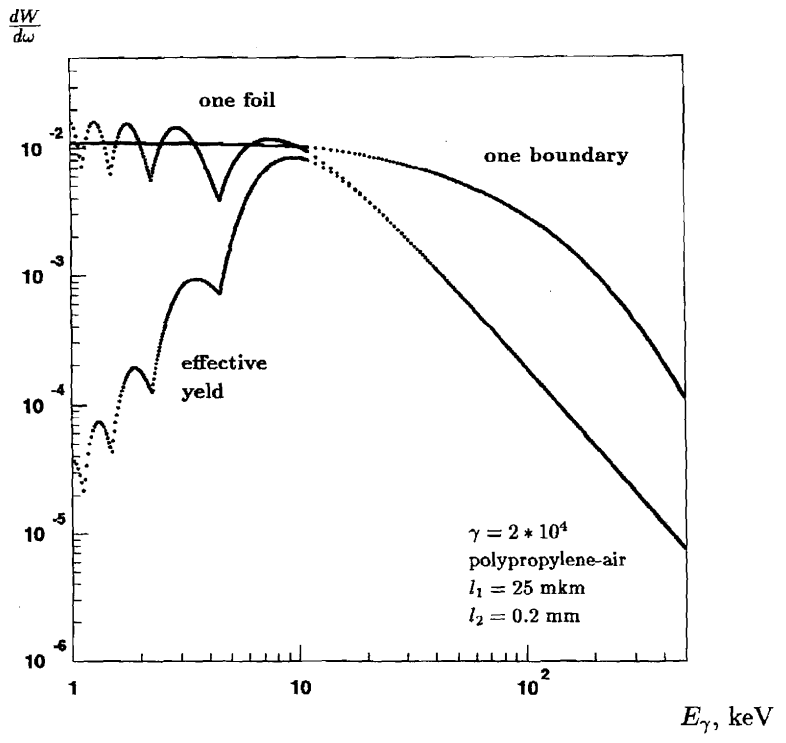

Figure 2. The computed differential yield per interface, as a function of TR photon energy.

$$Z_{1,2} = \frac{4c}{\omega}\left(\frac{1}{\gamma^2} + \theta^2 + \frac{\omega_{1,2}^2}{\omega^2}\right)^{-1} \tag{5}$$

The size of formation zone depends on the frequency of the radiation and the angle of emission. Physically, the formation zone is the distance along the particle trajectory in a given medium after which the separation between particle and generation photon is of the order of the photon wavelength. In this case the intensity of the radiation deteriorates if the thickness of the foil is smaller than a critical value Z. This minimal thickness correspond to the path length where the phase difference of the particle field and the radiation field becomes unity. Particle field and radiation field have to decouple which correspond to the minimum distance inside the foils required for the electromagnetic field of the particle to reach its new equilibrium value.

The next effect is a change in the spectral intensity distribution. For a single foil the amplitudes for the radiation at the transition $\omega_1 \rightarrow \omega_2$ is of the same order as for the transition $\omega_2 \rightarrow \omega_1$ with just the sign altered. The interference effect giving rise to minimum and maximum correspondence by the equation. This effect is shown on Fig. 2. As a consequence of the formation zone effect the cut of frequency is $\omega < min(\gamma\omega_2, l_2\omega_2^2/2)$. As another important consequence the mean radiated energy W ceases to increase linearly with γ but only logarithmically for $\gamma > l_2\omega_2/2$ and vacuum ($\omega = 0$). For $\omega \neq 0$ the frequency cut off will lead to saturation of the emitted radiation for $\gamma > \gamma_{max}$ with $\gamma_{max} = \frac{l_2\omega_2^2}{2\pi\omega_1^2}$.

The needed the finite thickness foil also lead to another problem, namely the reabsorption of the radiation emitted by the foil material itself. The equations has therefore to be modified:

$$\frac{d^2W_N}{d\theta d\omega} = \frac{d^2W}{d\theta d\omega} 4sin^2\left(\frac{l_1}{Z_1}\right) \frac{sin^2[N(l_1/Z_1 + l_2/Z_2)]}{sin^2(l_1/Z_1 + l_2/Z_2)} \left|\frac{1 - C^N}{1 - C}\right|^2 \tag{6}$$

$$C = exp(il_1/z_1 + il_2/z_2 - l_1\sigma_1 - l_2\sigma_2), \tag{7}$$

where σ_i - are the absorption cross section of the two materials.

For the energy range in question the absorption is dominated by the photoelectric effect. The absorption increases as Z^4/ω^3, while the TR total energy is roughly proportional to the plasma frequency ω_p of the material, which varies as $Z^{1/2}$. Therefore, if we want to increase the number of photons from the stack, it is preferable to use foils with small Z as radiator material. The

effective yield for a typical foil material polypropylene with the effect of absorption is shown in Fig. 2.

The brief summarize of parameters of TR radiator in simplified forms can see in [7], the influence of the main radiator parameters on the observed spectral response and total yield:

- **foil thickness** $\omega_{max} \propto l_2$

  a thicker foil leads to a harder spectrum. But since $W \sim \sharp$ of interfaces reabsorption of TR occurs which again is $\sim l_2$;

- **foil spacing** $\gamma_s \sim l_1$

  which determines saturation and has to be chosen according to the γ range in experiment. But for efficient TR production:

$$l_1 \geq Z_1 = \frac{2c\gamma^2}{\omega}\left(1 + \frac{\omega_1^2\gamma^2}{\omega^2}\right)^{-1} \tag{8}$$

- **radiator material** $W_0 \propto (\omega_1 - \omega_2)^2$

  ω_2 large $\rightarrow$ many electrons/cm^3 $\rightarrow$ high density, but reabsorption should be kept small $\rightarrow$ low Z material.

  Typical material for the TR radiator are mylar, CH_2 carbon fibers, lithium.

Practically the transition radiation (X-ray) emitted from a radiator can not be separated from the particle in time or space and detection of transition radiation as and any X-ray detection is defined as registration TR photons on top of a large background due to ionization loss of the charged particle in sensitive volume. In this case the X-ray detector has to consist of thin layer of high Z material thick enough to allow sufficient absorption of the X-ray but thin enough to limit the ionization loss. The mixture of a heavy noble gas (usually Xe) used as sensitive volume for detection transition radiation. While the absorption of a transition radiation gives rise to a very localized charge cloud the ionization seems almost equally distributed over the active depth of the detector. However, the ionization signal is composed of the signal from δ-electrons which themselves create charges clusters proportional to their energy. The large widths of ionization losses distribution observed in thin gas layers are due to the fluctuation of the number and energy of these δ-electrons. In particular, high energy δ-electrons give rise to a long tail of

the ionization loss distribution which will turn out to be the limiting factor for clean observation of the transition radiation.

The essential aspect of transition radiation detection is signal processing. So far two methods of signal processing have been mainly used. The first method (Q-method) uses the classical integration of the full charge deposited in a X-ray detector, disregarding the differences between TR signal and background (dE/dx). The second method (N-method) makes used the spatial distribution of signal and background along the track of particle. It relies on the separation of charge clusters in time steming from TR and dE/dx, which is related to a spatial mapping of the full signal distribution along the track of particle in sensitive volume. Imposing the threshold of a few keV to the charge of the TR hits collected should lead to a large reduction of background. Counting cluster above a given threshold also have advantages that the distributions of of signal and noise are following a Poisson distribution which exhibits much smaller tails than the ordinary dE/dx distributions tail.

3.2 Particle identification using Transition Radiation.

Electron identification makes use of the difference in energy deposited in detector by hadrons and electrons, and in particular of the higher tail above given threshold. The hadron rejection coefficient R, corresponding to a threshold value of TR hits is the ratio of efficiencies ε of two types of particles at the fixed value of number of TR hits.

$$R = \frac{\varepsilon_\pi}{\varepsilon_e} \tag{9}$$

The hadron rejection is calculated by counting the number of transition radiation hits (i. e. hits with energy more than given threshold). Events with low number of TR hits were rejected, thus leading to a hadron contamination which was a function of the chosen electron efficiency.

4 Monte Carlo program for Transition Radiation Simulation.

4.1 TR photon production

We have used the differential energy distribution for TR-photons emission from a particle with a Lorentz factor γ interacting with a TR radiator. The

TR radiator used in calculation is defined as multilayer stack of radiator foils with parameters: foil thickness, foil spacing.

The simulation of the TR photon production take into account the relative position of each foil and its thickness in order to add the complex electric field amplitudes correctly and reproduce interference effects [8],[9]. The algorithm is based on a calculation developed by G.Garibian et al [10].

- the number of TR photons is extracted for each event according to a Poisson distribution;
- to each photon is assigned energy according equation (6);
- photoabsorption process included the TR photon absorption by atom in TR radiator and gas of detector and secondary processes of eject of electrons from the K or L shell. The remainder of the energy appears as Auger electrons or fluorescence photons.

The other type of TR radiators - foil , carbon fibers is simulated using the procedure in which the irregular structure can be parameterized in terms of N layers of average thickness separated by an average spacing. Normalization factor corrected on the experimental results taken from test measurements in DESY HERA-B [18].

4.2 Energy deposit in the detector

The Monte Carlo simulation of the total energy deposition in the detector takes into account the TR photon absorption in sensitive gas volume and the contribution of the ionization process including the simulation of δ ray in gas volume. The energy deposited by charge particle in a medium is well reproduced by Landau distribution only if the material thickness is large than $2\beta Z$, and Landau theory can not be applied for thin gas layers [11]. The ionization energy loss were simulated using the calculation of V.Ermilova et al [12] for the spectrum of energy transfers of a charged particle in a thin gas layer, according to the basic conditions:

- the number of primary collisions of particle fluctuates according to the Poisson distribution;
- energy transfers in individual primary collisions are distributed according to spectrum from [12] ;
- the energy loss within gas layer is a sum on independent energy transfer.

4.3 Addition features of simulation program.

- A detailed electric field map used in order to calculate drift velocities as a function of the position in the drift chamber including the space charge effect.
- The simulation also taken into account the characteristic of the front-end electronics preamplifiers, shaping amplifiers and discriminator. Electronics noise, pedestal fluctuations and digitalization can also included in simulation.
- The simulation program is organized in order TR simulation library and compatible with GEANT Detector Description and Simulation Tool.

5 Detector description and results.

Transition Radiation Detectors HERA-B experiment - Study CP violation in the B system using an Internal Target at the HERA Proton Ring, is based on the new straw design - sandwich structure, where straw proportional counters embedded in TR radiator [13]. This structures are called "fine sampling TRDs" consist from many thin TR radiators and many X-ray detectors layers, which provide frequent measurement of TR photons. This structure already suggests the possibility of continuous tracking where the large number of detection planes is used to provide many space point for track reconstruction.

Total length of the Transition Radiation Detector along the particle beam is 76 cm. The total quantity of material along the trajectory in TRD are limited in order to reduce the interaction of particles with the material of the detector and was required to be less than 0.1 of a radiation length. The TR radiators are study to application in HERA-B are CH_2 Foam radiator [6], polypropylene fibre radiator [14]. Number of TR radiator + straw tubes layers in TRD are 32. The proportional straw tubes for transition radiation detector are prepared from a Kapton film containing a conductive layer on one side (1000 - 3000 $\AA$ Al + 4 μm Carbon - loaded Kapton) and thermoplastic polyuretane layer 3 μm on the other side. The total resulting straw wall thikness is about 60 μm. The triple mixture $Xe(70\%) + CF_4(20\%) + CO_2(10\%)$ proved to be very stable over a board range of operation voltages and demonstrated a linear responce to incident photons over a wide range of energies. At high gas gain ($2.5 * 10^4$) this mixture operates in the limited streamer mode

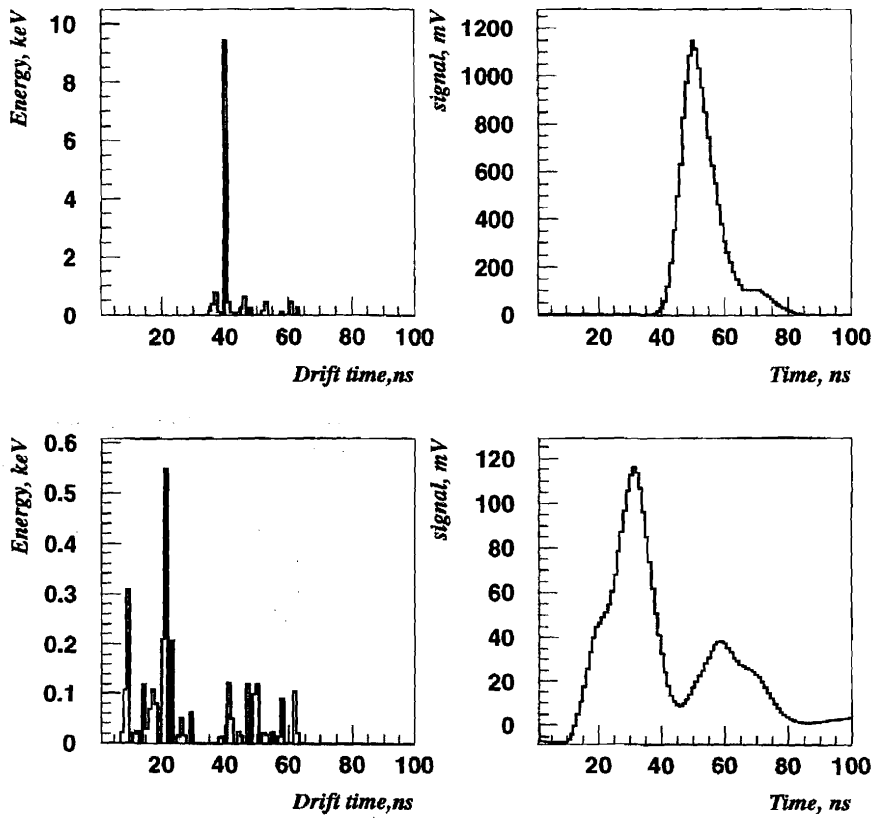

Figure 3: TR hits and Primary collision simulation and corresponded electronics signals for electron and pions 20 Gev/c.

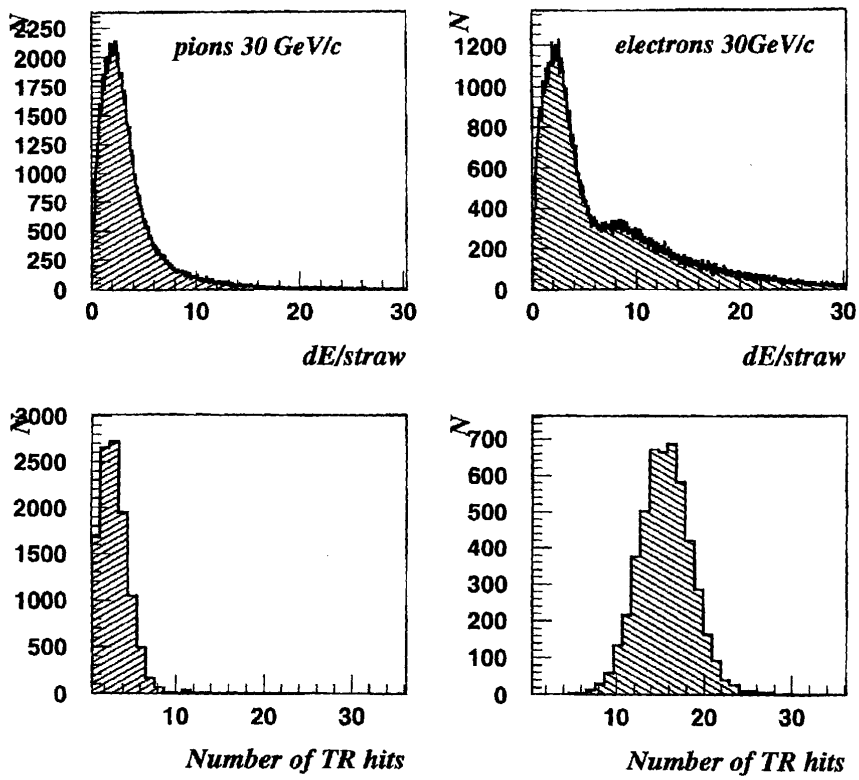

Figure 4. The energy distribution for a Straw tubes and TR hits distribution for pions and electrons 30 GeV/c.

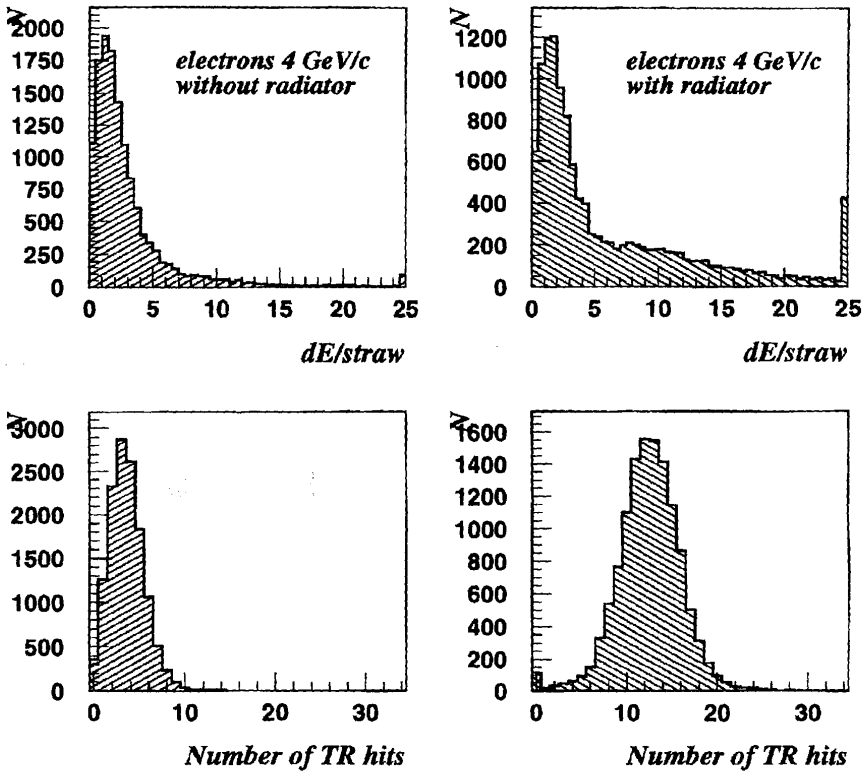

Figure 5. The experimental energy distribution for a Straw tubes and TR hits distribution with and without TR radiator (polypropylene fibre).

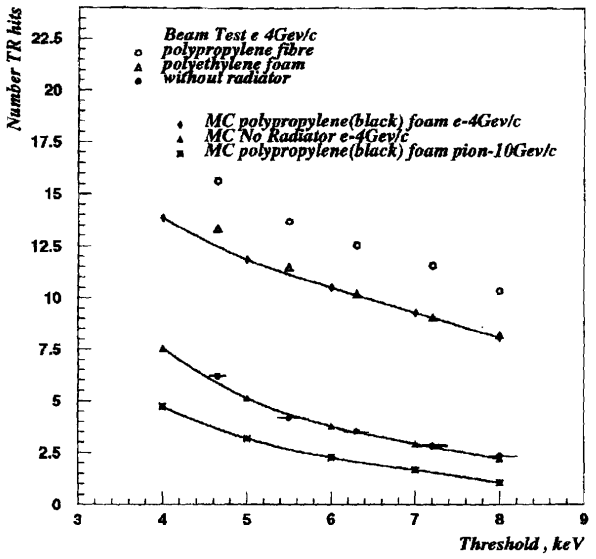

Figure 6. The number of TR hits vs threshold for different TR radiators as measured in a test beam, and comparison with Monte Carlo predictions (solid line).

without sparking and therefore is quite safe from point of view of breakdown. The total electron drift time of about 60 ns [15]. Methods used for particle identification is N-method of counting TR hits.

On the Fig. 3 is shown the results of simulation of primary collision distribution, energy deposition in straw tube gas with using the real dependence of drift velocity vs electric field inside straw tube, and electronics signal simulation using the realistic response of electronics.

The distribution of total energy loss in straw proportional tubes for electrons and pions with energy 30 GeV/c is shown on Fig. 4a. TR photons gives a long tail in the right side of energy spectrum and increase the number of hits above given threshold for N-method analysis as can see on Fig. 4b. The figure shows the predictions for the TR photon hits produced by the incident 30 GeV/c electrons and pions for threshold of 5.5 keV. This distributions used in N-methods of TR hit counting.

6 Results of TRD prototype test.

The important point of developing the Monte Carlo simulation is the confirmation that the predicted results correctly describe the response of TRD. The TRD prototype has 32 layers each consisting of a radiator followed by a straw rows for X-ray detection (straw diameter of 6 mm and length of 120 mm each), aligned along the insident beam direction. Each layer consist of four straws which are glued together and have joined anodes connected to the front-end electronics. All layers has been shifted relatively first layer in proportional 3/8 of diameter straw. The space between straw rows $\sim$ 40 mm was used to place radiator. The straws were operated with triple gas mixture $Xe(70\%) + CF_4(20\%) + CO_2(10\%)$. The test beam experiment with TRD prototype has been performed at the T24 beamline at DESY and used a secondary beam of electrons with momentum - 4 Gev/c. The estimation of electron/hadron rejection was made on base mesurements perfomance of prototype with and without TR radiator. On Fig. 5 you can see the energy distribution for a Straw tubes and TR hits distribution with and without TR radiator (polypropylene fibre) from experimental results of beam test of TRD prototype. On Fig. 6 is shown the experimental results of beam test of TRD prototype - dependence of number of TR hits vs threshold for two types of TR radiators and without TR radiator [18].

7 TRD performance in HERA-B spectrometer.

The full MC description of TR process was introduces in common MC HERA-B frame - ARTE. The simulation of performance was done on base of genereted events are produced for main goals of HERA-B experiment. The fragment of HERA-B set up near the TRD is shows on Fig. 7. The results taken from full Monte Carlo GEANT simulation of HERA-B experiment for events $B^0 \rightarrow J/\psi K_s^0$ decays with background of 4 mbias are shown on Fig. 8.

Fig. 8 shows the hadron rejection factor for such a case calculated for 5 interactions per bunch using the full HERA-B GEANT simulations and dedicated library for ionization losses and TR photons simulation normalized on the TRD prototype test data. On Fig. 8 you can see the hadron rejection of $\sim$ 17 is achievable even for very high electron efficiency of 98% for electrons from J/ψ decays.

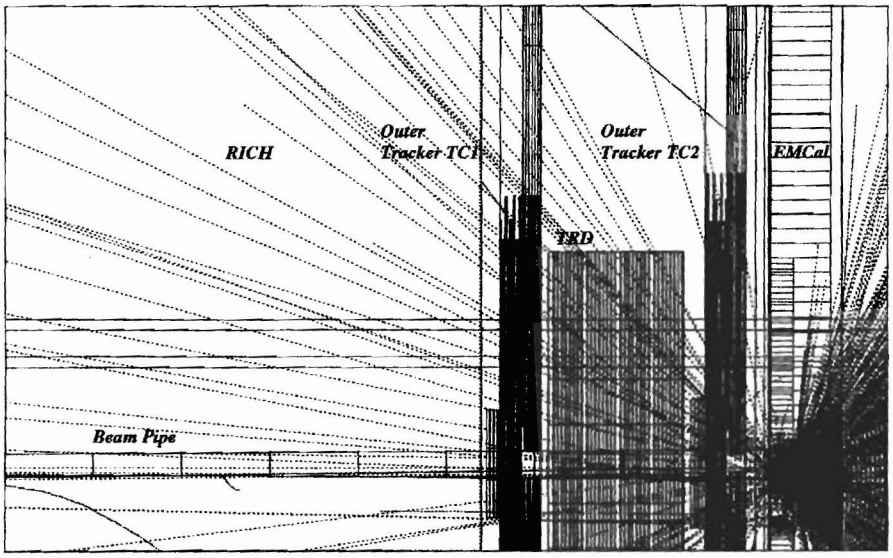

Figure 7. The view of TRD structure as straw tubes layers embedded in TR radiator in HERA-B experiment.

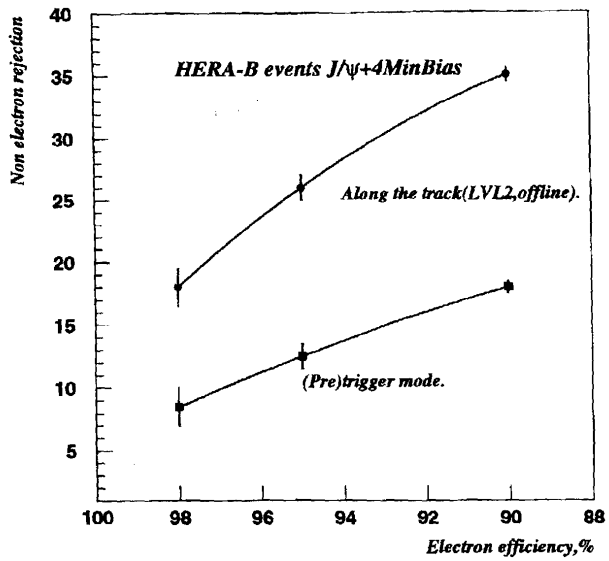

Figure 8. Rejection factor for the HERA-B GEAN simulation events including simulation of TRD response.

8 Conclusion.

Monte Carlo simulation of transition radiation has been made on basis of model compatible with GEANT - Detector Description and Simulation Tool. The Monte Carlo transition radiation simulation describes the process of charge particle passing through the medium taking into account the transition radiation TR photons including their energy and angular spectra, TR photon absorption including the secondary fluorescent X-ray for the Xe from K,L shell, absorption of TR photons in radiator and materials of detector. Detailed simulation of ionization losses in thin gas layers, take into account the primary collisions distributions, calculation the energy deposit in gas layer, electron drift time with real dependence of drift velocity vs electric field, electronics signal. We have compared the experimental results obtained in a test full length prototype of the TRD HERA-B with a Monte Carlo simulation.We obtained the good agreement between the Monte Carlo simulation and the experimental data. The Monte Carlo simulation of transition radiation are

used for full GEANT simulation of HERA-B experiment.

Acknowledgments.

We are very grateful to the HERA-B Collaboration and especialy to professor B.Dolgoshein for his participate in ours scientific activity and for many very fruitful discussions.

References

[1] I.I.Bigi et al. *CP Violation: Advanced Series on Direction in High Energy Physics*, ed. C. Jarlskog (World Scientific, Singapore, 1988).

[2] T.Lose et al., *An Experiment to Study CP Violation in the B System Using an Internal Target at the HERA Proton Ring*, Proposal,DESY-PRC 94/02, Hamburg, 1994.

[3] I.Frank,V.Ginzburg *J. of Phys.*, 9, 353, (1945).

[4] G.M.Garibian, *Zh. Eksp. Teor. Fiz.* 33, 1403, (1957).

[5] M.Cherry at al., *Phys. Rev.* D **10**, 3594 (1974).

[6] B.Dolgoshein., *Nucl. Instrum. Methods* A **326**, 434 (1993).

[7] S.Paul, *Particle Identification Using Transition Radiation Detectors*, CERN/PPE 91-199, 1991.

[8] V.Saveliev, *Proceeding of the International Conference on Computing in High-energy Physics (CHEP97)*, Berlin, Apr. 1997.

[9] V.Saveliev, *Nucl. Instrum. Methods* A **408**, 289 (1998).

[10] G.Garibian at al., *Nucl. Instrum. Methods* A **125**, 133 (1975).

[11] Y.Ducros at al., *Nucl. Instrum. Methods* A **277**, 401 (1989).

[12] V.Ermilova at al., *Nucl. Instrum. Methods* A **145**, 555 (1977).

[13] E.Hartouniet al., *An Experiment to Study CP Violation in the B System Using an Internal Target at the HERA Proton Ring*, Design Report, DESY-PRC 95/01, Hamburg, 1995.

[14] TRD ZEUS Group, *Nucl. Instrum. Methods* A **323**, 135 (1992).

[15] B.Dolgoshein at al., *Nucl. Instrum. Methods* A **294**, 473 (1990).

[16] J.D. Bjorken and I. Dunietz, *Phys. Rev.* D **36**, 2109 (1987).

[17] C.D. Buchanan et al, *Phys. Rev.* D **45**, 4088 (1992).

[18] V.Egorytchev et al., *Experimental results for test run with prototipe of TRD HERA-B*, MEPhI 001-99, 1999.